Dynamics of Dirac Fermions in Topological Insulators

R. Hammer[1], C. Ertler[1], W. Pötz[1], and A. Arnold[2]

[1]Uni-Graz
Institut für Physik (Theory Division)
Universitätsplatz 5, 8010 Graz, Austria

[2]TU-Wien
Institut für Analysis und Scientific Computing
Wiedner Hauptstr. 8, 1040 Wien, Austria

email: rene.hammer@uni-graz.at

Abstract

We study the coherent dynamics of Dirac fermions on the surface of topological insulators in one and two space dimensions. Our finite difference scheme can handle space– and time–dependent mass and potential terms and is complemented by newly–developed transparent boundary conditions. Dirac fermions show interesting dynamical behavior based on effects, such as negative refraction and therefore 'superlens' focusing on a Klein–step or the formation of chiral channels along domain boundaries where the effective mass changes sign.

1 The Physics

Motivated by recent theoretical and experimental progress of 3D topological insulators (TI) we investigate theoretically the dynamics of Dirac fermion wave packets on their 2D surfaces. Briefly stated, the ingredients for a TI state are an insulating bulk material with strong spin–orbit coupling and the conservation of time–reversal (TR) symmetry[1, 2]. Following a bulk–boundary correspondence principle, this leads to topologically protected gapless surface states which can be described by an effective 2D field theory, and whose texture has been seen in spin–ARPES [2]. The electron Hamiltonian is analogous to that of the 2D (2+1) Dirac equation $H = [v_F\vec{p} + e\vec{A}_{eff}]\vec{\sigma} + M\sigma_z - eV$. However, one can generate a space–dependent mass M term due to the coupling to a ferromagnetic layer which breaks TR symmetry. The Pauli–matrices corresponding to real spin and the possibility of the creation of a rather large mass term (order of 10 meV) are promising differences compared to graphene.

2 The Numerical Scheme

For our simulations we use a staggered–grid finite difference scheme which can handle fully space– and time–dependent mass and potential terms. In the 1D (1+1) case it is dispersion preserving for a certain ratio of time– to space–step, preventing the notorious fermion doubling problem. For the full 2D scheme it is dispersion preserving in the main directions. In Schrödinger form and using the standard Pauli matrices, $\boldsymbol{\sigma_r}$, $\boldsymbol{r}= x, y, z$, the Dirac equation in 2D in normalized units reads:

$$i\partial_t\boldsymbol{\psi}(x,y,t) = \hat{H}\boldsymbol{\psi}(x,y,t)\ ; \quad \hat{H} = m\sigma_z - i\partial_x\sigma_x - i\partial_y\sigma_y - V$$

With our staggered–grid leap–frog discretization (see Fig.1) and the notation $\boldsymbol{\psi}(x_j, y_k, t_n) = \boldsymbol{\psi}^n_{j,k} = (u^n_{j,k}, v^n_{j,k})$, where n and j, k are, respectively, the discrete time index and space indices, we obtain:

$$\frac{u^{n+1}_{j,k} - u^n_{j,k}}{\Delta t} + i(m - V)\frac{u^{n+1}_{j,k} + u^n_{j,k}}{2} + \frac{(v^n_{j,k-1} - v^n_{j-1,k-1}) + (v^n_{j,k} - v^n_{j-1,k})}{2\Delta x} - i\frac{(v^n_{j-1,k} - v^n_{j-1,k-1}) + (v^n_{j,k} - v^n_{j,k-1})}{2\Delta y} = 0$$

$$\frac{v^{n+1}_{j,k} - v^n_{j,k}}{\Delta t} - i(m + V)\frac{v^{n+1}_{j,k} + v^n_{j,k}}{2} + \frac{(u^{n+1}_{j+1,k} - u^{n+1}_{j,k}) + (u^{n+1}_{j+1,k+1} - u^{n+1}_{j,k+1})}{2\Delta x} + i\frac{(u^{n+1}_{j,k+1} - u^{n+1}_{j,k}) + (u^{n+1}_{j+1,k+1} - u^{n+1}_{j+1,k})}{2\Delta y} = 0$$

Stability and dispersion analysis for this linear system was done by Fourier analysis. It reveals that for $m, V \in \mathbb{R}$ the norm $||\psi||_2$ is preserved and the method (for $\Delta t = \Delta x$) reproduces the exact relativistic dispersion relation $\epsilon = \sqrt{m^2 + p^2}$ in the main directions (x, y).

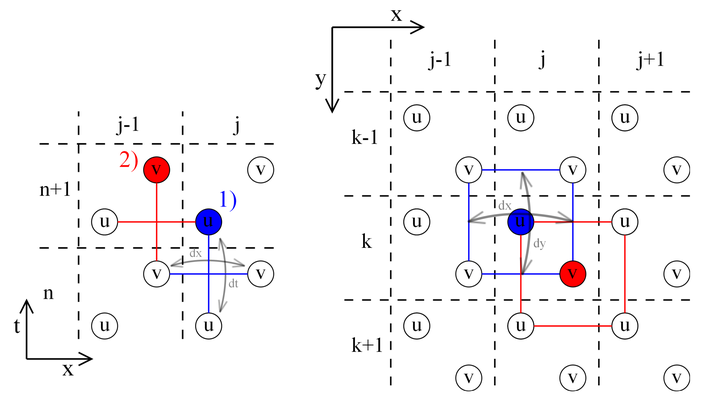

Fig. 1: Leap-frog staggered-grid scheme. Left picture shows time-stepping where 1) the new u–components (blue) are computed by the previous u and the difference of old v–values. 2) Then knowing u at t_{n+1} the new v at t_{n+1} (red) are computed using these values. The mass m and potential V enter the scheme in a Crank–Nicolson time averaging over current– and previous–time values. The right part of this figure shows the scheme for the spatial derivatives.

3 The Boundary

For the simulation in a finite space domain we incorporate discrete transparent boundary conditions (DTBCs) which ensure that the solution from a finite domain is equal to that for the full space problem with position–independent coefficients in the outside regions. In 1D this is done exactly by analytically solving the discretized exterior domain with a Z-transformation, following earlier work on the Schrödinger equation [3]. A generalization of these DTBCs to 2D is subject of further work. For our simulations here we have used preliminary approximate TBCs (called absorbing boundary conditions ABCs) instead. One possible choice is using ABCs for the wave equation $\partial_x = \pm\partial_t$ (or higher order approximations) [4] in discretized form. They have an absorption quality dependent on the angle of incidence. Remark: Because they are a discretization of continuous TBCs such ABCs cannot suppress spurious waves resulting from fermion doubling.

Another possibility to obtain ABCs for our difference scheme is to use an imaginary potential $\mathrm{Im}(V) \neq 0$. This acts as a dissipation term which violates conservation of norm $||\psi||_2$. We pragmatically build an absorbing layer with $\mathrm{Im}(V)$ around our domain. Remark: Caution, this is a special property of the staggered–grid leap–frog scheme and does not work for an arbitrary finite difference method.

4 Numerical Results

In the figures below we show the wave–packet dynamics for, initially Gaussian, wave packets. Shown is the real part (of one spinor component) of the wave function. For the Fermi–velocity we use $v_F = 6.2 * 10^5$ m/s [1]:

a) Negative refraction at a Klein step (row (a)): The first row shows a massless Dirac electron with average energy of $E = 45$ meV encountering a static Klein-step of height $V = 100$ meV with an average angle of incidence $\theta \approx 27°$. Because of $m = 0$, group and phase velocity are equal to v_F. In the region where $V = 0$ they also have the same direction, whereas in the $V = 100$ meV region, they point in opposite direction. What follows is negative refraction which shows up in our simulations.

b) Electron superlens focusing (row (b)): We consider a Klein step of height $V = 100$ meV and prepare the initial wave packet with $E = 50$ meV, well localized in space, so that there is high uncertainty in its direction of propagation. We demonstrate what has been predicted for graphene before[5]: the Klein–step redirects the Dirac fermion wave packet towards a focal point. Such properties can be exploited to construct quantum interference devices which we want to investigate in future research.

c) Electron interferometry between chiral channels (row (c)): The last row shows a Dirac fermion propagating in chiral channels which form at magnetic domain boundaries when the effective mass changes its sign. Because of the chiral nature of these edge–channels positive mass regions (+) can only be circled clockwise, while negative mass regions (−) can only be circled counterclockwise. Constructive interference (seen in the last two figures of row (c)) enhances transmission via the exit channel to the right. By making one interference path longer (by making a suitable mass domain slightly bigger) destructive interference for the exit channel can be achieved. Then the fermion is trapped inside the double–ring structure. This means that one can switch between perfect transmitting and insulating behavior. When the wavelength is changed by applying a potential, e.g. on the upper half–plane, quantum beating occurs.

5 Acknowledgments

This research was funded by the Austrian Science Fund (FWF): I 395-N16

References

[1] X.L. Qi, S.C. Zhang, Rev. Mod. Phys. 83 (2011), 1057-1110.

[2] Y. Xia, et al., Nature Physics 5 (2009), 398 - 402.

[3] A. Arnold, M. Ehrhardt, I. Sofronov, Comm. Math. Sci. 1 (2003), 501-556.

[4] B. Engquist, A. Majda, Proc. Natl. Acad. Sci. 74 (1977), 1765-1766.

[5] V.V. Cheianov. et al., Science 315 (2007), 1252-1255.